PROCEEDINGS OF SCIENCE

A TES system for ALPS II - Status and Prospects

José Alejandro Rubiera Gimeno,[a,*] **Friederike Januschek,**[a] **Katharina-Sophie Isleif,**[a,**] **Axel Lindner,**[a] **Manuel Meyer,**[b] **Gulden Othman,**[c] **Christina Schwemmbauer**[a] **and Rikhav Shah**[d,***]

[a] *Deutsches Elektronen-Synchrotron DESY, Notkestr. 85, 22607 Hamburg, Germany*
[b] *CP3-Origins, University of Southern Denmark, Campusvej 55, 5230 Odense M, Denmark*
[c] *Institut für Experimentalphysik, Universität Hamburg (UHH), Notkestr. 85, 22607 Hamburg, Germany*
[d] *Institute for Physics, Johannes-Gutenberg-Universität (JGU), Staudingerweg 7, 55128 Mainz, Germany*
[**] *now at Helmut-Schmidt-Universität (HSU)*
[***] *now at Universität Hamburg (UHH)*
E-mail: jose.rubiera.gimeno@desy.de, friederike.januschek@desy.de, katharina-sophie.isleif@desy.de, axel.lindner@desy.de, manuel.meyer@desy.de, gulden.othman@desy.de, rikhav.shah@desy.de, christina.schwemmbauer@desy.de

The Any Light Particle Search II (ALPS II) is a Light-Shining-through-a-Wall experiment operating at DESY, Hamburg. Its goal is to probe the existence of axions and axion-like particles (ALPs), possible candidates for dark matter. In the ALPS II region of interest, a rate of photons reconverting from axions/ALPs on the order of 10^{-5} cps is predicted by some astrophysical hints. A first science run at lower sensitivity based on a heterodyne detection method was successfully started in May 2023. The design sensitivity is expected to be reached in 2024. A complementary science run is foreseen with a single photon detection scheme. This requires a sensor capable of measuring low-energy photons (1.165 eV) with high efficiency and a low dark count rate. We investigate a tungsten Transition Edge Sensor (TES) system as a photon-counting detector that promises to meet these requirements. This detector exploits the drastic change in resistance caused by the absorption of a single photon when operated in its superconducting transition region at millikelvin temperatures. To achieve the required sensitivity, implementing the TES into the ALPS II experiment needs to be carefully optimized. In this work, we present the progress on measurements for the characterization of our system and data analysis for background reduction.

*** *The European Physical Society Conference on High Energy Physics (EPS-HEP2023),* ***
*** *20–25 August 2023,* ***
*** *Universität Hamburg, Hamburg, Germany* ***

[*] Speaker

1. Introduction

Axion-like particles (ALPs) are pseudo-scalar or scalar bosons postulated by Beyond Standard Model theories [1]. Light-shining-through-a-wall (LSW) experiments [2, 3] represent a model-independent approach to search for these particles, investigating the interaction between axions/ALPs and photons, characterized by the coupling $g_{a\gamma\gamma}$. In the LSW approach, a photon is converted into an ALP by interacting with a magnetic field (Primakoff effect) and vice versa (Sikivie effect).

The Any Light Particle Search II (ALPS II) is an LSW experiment located at the Deutsches Elektronen-Synchrotron (DESY) [4]. As a second-generation experiment, it will enhance the sensitivity on the coupling by a factor of 10^3 compared to previous similar experiments [5, 6], expecting to reach $g_{a\gamma\gamma} = 2 \cdot 10^{-11}$ GeV^{-1}. This value is motivated by astrophysical anomalies, e.g. stellar evolution [7]. Given the experimental conditions and the target sensitivity, the probability of the photon-ALP-photon process, assuming this coupling, is still very low. Starting from a rate of 1064 nm photons for conversion to ALPs equivalent to 30 W and assuming $g_{a\gamma\gamma} = 2 \cdot 10^{-11}$ GeV^{-1}, only 10^{-24} W would be converted back to photons, which means in the order of 10^{-5} cps or one reconverted photon per day [8]. Two detection schemes have been designed to overcome the challenge of measuring the reconverted photons: heterodyne detection (HET) [9] and single photon detection. The HET scheme is already implemented, and the ALPS II initial science run is ongoing using this system. The single photon detection scheme will be used as confirmation/cross-check or in case it can provide better performance than the HET.

For a single photon detector, it is required to be sensitive to 10^{-5} cps of photons with 1.165 eV energy within 20 days of data taking, and to have good energy resolution to reject the remanent green light from the ALPS II laser used for cavity monitoring [4]. Furthermore, to aim for a 5σ significance ALPs observation with ALPS II, a detection efficiency higher than 50 % and low background rates of less than $7.7 \cdot 10^{-6}$ cps [10] is necessary. A Transition Edge Sensor (TES) is under investigation as a very good candidate to fulfill these requirements. Measurements for noise characterization, energy resolution, background rejection, efficiency, and energy calibration are in progress [11]. In the next sections, the efforts on the optimization of energy resolution and measurement of the system detection efficiency will be discussed.

2. TES setup

A TES is a cryogenic microcalorimeter operated in the transition region between superconducting and normal conducting states [12]. It reacts to energy depositions with an abrupt change in resistance, producing a measurable signal. In our case, this is realized with a tungsten microchip provided by the National Institute of Standards and Technology (NIST), USA, under study for its future use in the ALPS II experiment. It has dimensions of 25 µm × 25 µm × 20 nm, a critical temperature around 140 mK and it is sensitive to energies in the order of 1 eV. The signal produced in the TES as a consequence of energy deposition is measured as a voltage signal using a Superconducting Quantum Interference Device (SQUID) readout provided by Physikalisch-Technische Bundesanstalt (PTB), Berlin, Germany. The TES and the SQUID cold parts are placed inside a Bluefors dilution refrigerator at a base temperature of 25 mK [13].

Photons are sent to the TES via optical fiber from outside the cryostat. To characterize its response to the ALPS II working wavelength, we send in the light from a 1064 nm laser, which is highly attenuated to avoid the saturation of the sensor. The attenuation is tuned to prevent a large contribution of pile-ups in the sample that will be analyzed [14]. An example pulse from a 1064 nm photon in a window of 40 μs is shown in Fig. 1a.

We define *intrinsics* as the measurement of the background by decoupling the optical fiber from the detector [10]. Therefore, the TES is in the dark, protected from the exterior environment by the shields of the cryostat. In this condition and using the acquisition conditions as in the 1064 nm laser data taking, a trigger rate in the order of 10^{-2} cps is observed. In the *extrinsics* measurement, we measure the background by connecting the TES to the optical fiber, but leaving the other end of the fiber in the dark at room temperature [14]. We obtain a higher rate compared to the intrinsics due to an additional contribution assumed to be mainly from black body radiation from the lab which couples into the fiber.

3. Pulse shape analysis in frequency domain

The observed rate of triggered intrinsics events is too high for the ALPS II requirements. To counter this, a pulse shape analysis has been implemented using the function in Eq. 1 in a fitting procedure applied to the signal in a time window.

$$U_{ph}(t) = -\frac{2A}{\exp\left\{-\frac{1}{\tau_{rise}}(t-t_0)\right\} + \exp\left\{\frac{1}{\tau_{decay}}(t-t_0)\right\}} + V_0 \tag{1}$$

This function is obtained from a phenomenological approach and describes well the photon pulses [13]. The parameters A, τ_{rise}, and τ_{decay} define the shape of the pulse and are related to its amplitude, rise time, and decay time respectively. The parameters t_0 and V_0 correspond to the position of the pulse in the time window and the voltage offset. Cuts imposed on the fitting parameters in an intrinsic sample allowed the rejection of almost all background events, reaching a rate of $6.9^{+2.6}_{-1.5} \cdot 10^{-6}$cps [10] while keeping more than 90 % efficiency for 1064 nm photons, reflecting that the intrinsics sample contains pulses with an amplitude and shape different than the one for photons. These results have been further improved using machine learning techniques [15].

It is not likely that by using this method most of the additional contribution expected in the extrinsics background can be rejected, as it consists mainly of photons. Among the strategies to reduce this background, we are working on possibly filtering non-1064 nm photons in the cold and improving the energy resolution.

As suggested by the results using the Small Signal Theory (SST) [12], the time integral of a pulse is assumed to be proportional to the energy of the arriving photon. The energy resolution in our system is calculated as the ratio between the values σ and μ of a Gaussian function fitted to the distribution of computed time integrals from more than 500 pulses, as shown in figure 2a. In this case, the energy resolution is ER = (11.6 ± 0.2)%, equivalent to a Full Width at Half Maximum (FWHM) of 0.32 eV, larger compared to other sensors, e.g. 0.26 eV using a 1550 nm source [16].

We have developed a frequency domain-based analysis aiming to improve the energy resolution for 1064 nm photons. The SST predicts a piece-wise model for the TES response to a delta-function small energy injection.

$$U_{SST}(t) = \begin{cases} A\left(\exp\left\{-\frac{1}{\tau_+}(t-t_0)\right\} - \exp\left\{-\frac{1}{\tau_-}(t-t_0)\right\}\right), & t \geq t_0 \\ 0, & \text{else} \end{cases} \tag{2}$$

However, this piece-wise function, Eq. 2, is not suitable for the fitting procedure as it is not differentiable, making the fitting unstable [13]. The parameters A, τ_+, τ_-, and t_0 are analogous to the parameters A, τ_{rise}, τ_{decay} and t_0 in the phenomenological model.

$$\mathcal{F}[U_{SST}(t)](f) = -A(\tau_- - \tau_+)\frac{[1-(2\pi f)^2\tau_+\tau_-] - i2\pi f(\tau_+ + \tau_-)}{[1+\tau_+^2(2\pi f)^2][1+\tau_-^2(2\pi f)^2]}\exp\{-2\pi f i t_0\} \tag{3}$$

The Fourier transform (Eq. 3) of Eq. 2 is not piece-wise defined, and the parameters keep their physical meaning. The Eq. 3 is complex, as it has a real part and an imaginary part. Nevertheless, a fitting procedure can be implemented based on it. A Fast Fourier Transform (FFT) is applied to a time window of the data (Fig. 1a) to obtain its real part (Fig. 1b) and imaginary part (Fig. 1c). The magnitude of the noise extracted as in [14], is used to estimate the uncertainty that appears in figures 1b and 1c.

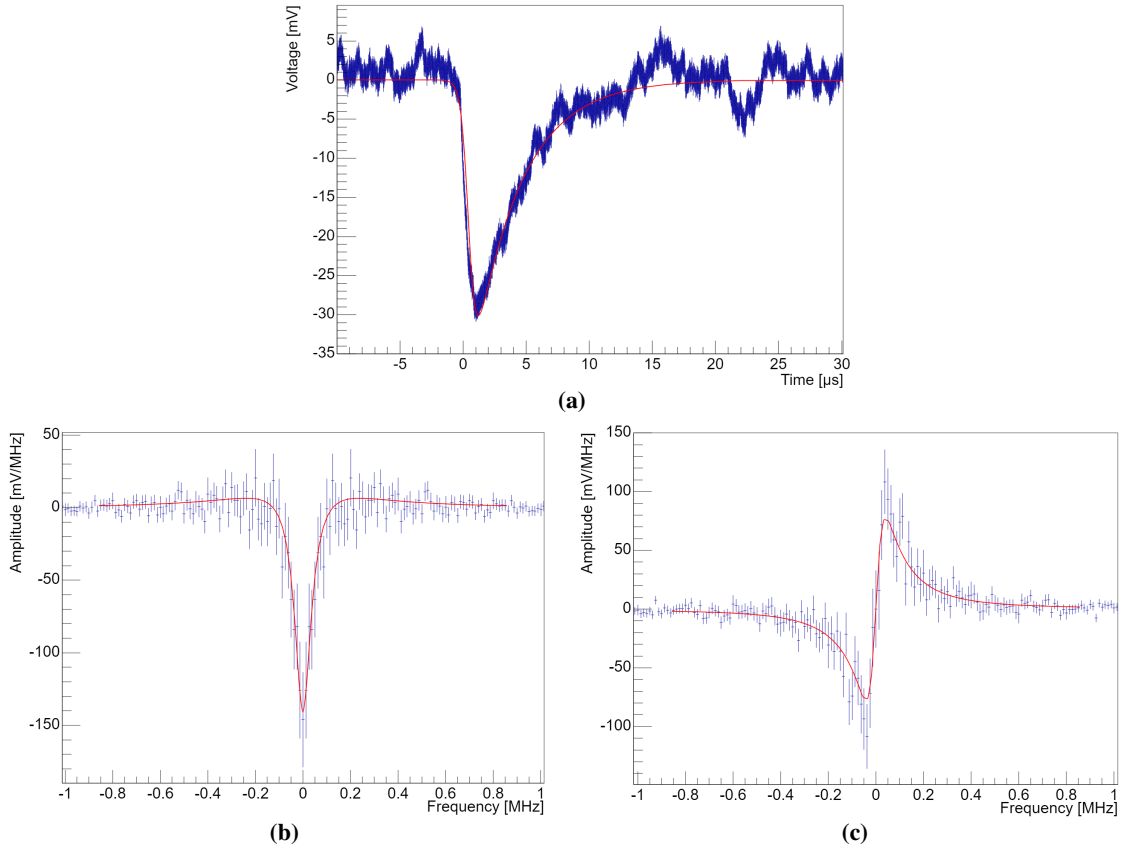

Figure 1: (a) Example of 1064 nm pulse in the time domain, (b) real part of the FFT fitted to the real part of Eq. 3, (c) imaginary part of the FFT fitted to the imaginary part of Eq. 3.

The time integral of the signal fitted in the frequency domain can be calculated, by definition, by evaluating Eq. 3 at zero. The result improves the energy resolution to ER = (10.3 ± 0.2)%

in the same dataset, with a FWHM of 0.28 eV, an improvement of approximately 10 %. Further optimization is made by calculating the pulse height $U_{SST}(t_{max})$ of the fitted signal in the frequency domain, using the parameters A, τ_+, and τ_-, where t_{max} is the solution of $U'_{SST}(t_{max}) = 0$. The computed distribution is shown in Fig. 2b. Following the same procedure as with the time integral, the resulting energy resolution is ER = (5.31 ± 0.06)%, with a FWHM of 0.15 eV. This represents an improvement by a factor of two compared to the previous result. A possible explanation for this improvement is that the pulse height receives a lower influence from the Brownian noise, which dominates the energy resolution for the pulse integral [14]. The maximum amplitude of the pulse is reached in 1 – 2 μs, therefore it is under the influence of high frequencies, where Brownian noise has a lower contribution.

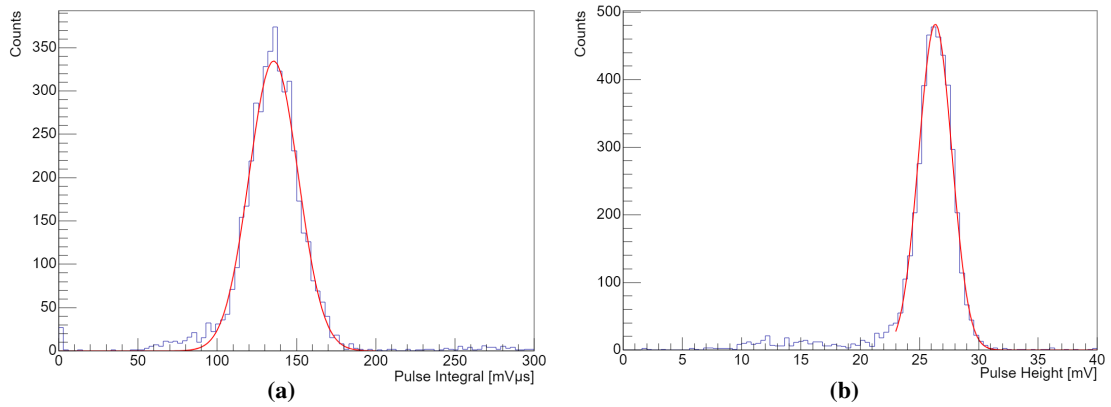

Figure 2: Histograms of the same set of 1064 nm pulses of the: (a) pulse integral with ER = (11.6 ± 0.2)%, FWHM = 0.32 eV, and (b) pulse height with ER = (5.31 ± 0.06)%, FWHM = 0.15 eV.

This analysis presents additional advantages. The Eq. 3 is linked to the SST, where the parameters A, τ_+, and τ_- are related to the TES physical parameters. Finding these parameters means that the TES parameters can be calculated from theory. Moreover, in the frequency domain, a photon signal is only dominant in a limited range of frequencies, and then the fit is only performed over this range, decreasing the number of points to be fitted. The fit is also done using one less parameter, as V_0 is only an offset in the zero frequency point. These last two factors contribute to a substantial reduction in the time required to perform the fitting procedure.

4. Efficiency measurement

As mentioned in section 1, a high detection efficiency of the TES is required to be suitable for the ALPS II experiment [4]. Higher efficiency allows a higher significance for an ALP observation with ALPS II, with the same rate of background events. We measure the efficiency of the TES system, as a first step in its characterization. This includes the coupling between the TES and the optical fiber used to propagate the light from outside the cryostat and the transmission in the fiber. In this value, the coupling to the ALPS II experiment and the analysis efficiency are excluded. Previous measurements done by NIST and PTB suggest that a 90% efficiency is reachable [17, 18]. We have designed a setup based on PTB's approach [19], using a traceable calibrated photodiode (calPD) as a power reference. The main challenge lies in the dynamic range of both detectors, as the

minimum power that can be measured with the calPD is in the order of 10^{-11} W, and the maximum power that can be measured in the TES before it saturates is in the order of 10^{-15} W.

A setup that overcomes this challenge is shown in Fig. 3. A 1064 nm laser injects 1 mW into an optical fiber. A 50/50 splitter sends a part of the power to a photodiode to monitor the laser, the other part is attenuated by several orders of magnitude to enter the dynamic range of the calPD. The 99% output of a 99/1 splitter is sent to the calPD, and the 1% goes to two electronic variable optical attenuators (VOAs), and then to the TES. The value of the voltage for the VOAs' attenuation is set, so that the signal at the TES presents the least amount of pile-up, but the attenuation of the system beam splitter / VOAs can still be measured with the calPD. With this configuration (Fig. 3), we measure the power at the calPD (P_{cal}) and the rate of photons that arrive at the TES (n_{TES}). The main advantage of using electronic VOAs consists of the reproducibility of the results, given that the attenuation is controlled by varying the voltage supplied to them. Moreover, this also allows us to reduce the attenuation to almost zero without unplugging the optical fibers that connect them, which can introduce additional uncertainties.

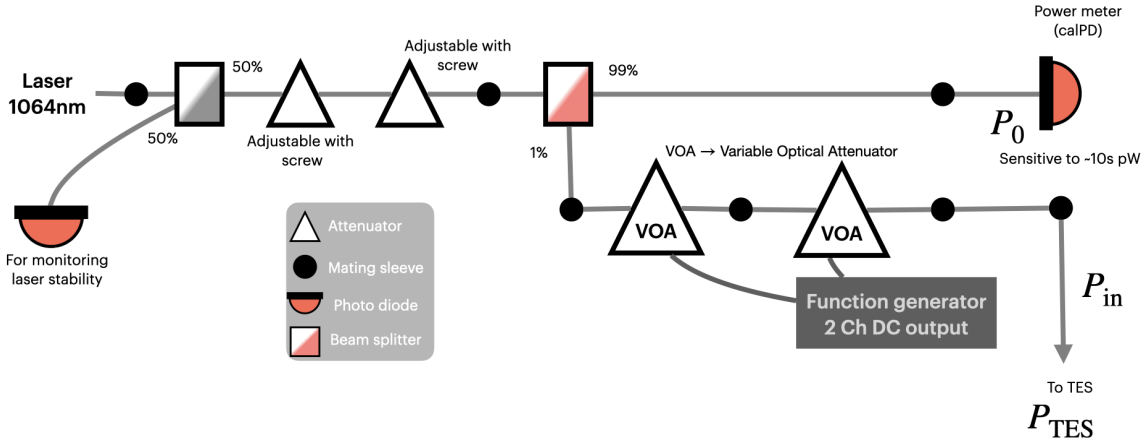

Figure 3: Scheme of efficiency measurement, as suggested in [11]. Configuration where the power is measured simultaneously at the photodiode (P_{cal}) and the TES (n_{TES}).

Afterward, we need to change the configuration in Fig. 3 to find the split ratio between the two outputs of the 99/1 beam splitter ε and the total attenuation in the TES line α. First, we change the attenuation of the fiber line coming from the laser, to get the calPD just below saturation (P_{calH}). Secondly, we connect the calPD to the other line instead of the TES. Then, we measure the power when the two VOAs are at minimum attenuation (P_{L0}), one at minimum and the other at the value used in the previous variant of the setup (P_{L1}), and vice-versa (P_{L2}).

The system detection efficiency (SDE) is calculated using Eq. 4:

$$\mathrm{SDE} = \frac{n_{TES} \cdot E_{1064nm} \cdot \varepsilon \cdot \alpha}{P_{cal}}, \quad \varepsilon \cdot \alpha = \frac{P_{calH} P_{L0}}{P_{L1} P_{L2}} \tag{4}$$

The measurement gives a preliminary result for a fiber-to-TES coupling efficiency greater than 80 %. Assessment of uncertainties and reproducibility of the results is in progress. Furthermore, the value of n_{TES} depends on the algorithm's accuracy used to locate 1064 nm pulses in a timeline. Therefore, a dedicated pulse-finding algorithm is under development.

5. Conclusions and outlook

ALPS II is expected to probe $g_{a\gamma\gamma}$ in a model-independent approach beyond present limits from astrophysics and helioscopes. It started data taking using a heterodyne-based detection scheme in May 2023. The TES is a good candidate for a single photon detection scheme to complement the current measurements with the HET detection system. This would be particularly important in case an ALP signal is observed. Furthermore, the TES could enhance the sensitivity of ALPS II if a better performance than the HET is reached. Towards these scenarios, the TES detection system is being characterized and optimized. Regarding this, an analysis in the frequency domain has been presented where an improvement by a factor of two in energy resolution was demonstrated, reaching an FWHM of 0.15 eV. Additionally, a measurement of the fiber-TES coupling efficiency was performed and the result exceeded 80%. Further investigation on uncertainties and reproducibility of the efficiency measurement is in progress. The feasibility of the TES for direct dark matter detection is also under study [20].

6. Acknowledgments

We would like to thank our ALPS collaborators, the National Institute of Standards and Technology, USA, for the TES devices and Physikalisch-Technische Bundesanstalt, Berlin, Germany, for the SQUID modules and helpful advice. Manuel Meyer acknowledges the support from the European Research Council (ERC) under the European Union's Horizon 2020 research and innovation program Grant agreement No. 948689 (AxionDM).

References

[1] A. Ringwald, *Axions and axion-like particles*, 1407.0546.

[2] A.A. Anselm, *Arion ↔ Photon Oscillations in a Steady Magnetic Field. (In Russian)*, *Yad. Fiz.* **42** (1985) 1480.

[3] K. Van Bibber, N.R. Dagdeviren, S.E. Koonin, A.K. Kerman and H.N. Nelson, *Proposed experiment to produce and detect light pseudoscalars*, *Phys. Rev. Lett.* **59** (1987) 759.

[4] R. Bähre, B. Döbrich, J. Dreyling-Eschweiler, S. Ghazaryan, R. Hodajerdi, D. Horns *et al.*, *Any light particle search II — Technical Design Report*, *Journal of Instrumentation* **8** (2013) T09001–T09001.

[5] I.G. Irastorza and J. Redondo, *New experimental approaches in the search for axion-like particles*, *Progress in Particle and Nuclear Physics* **102** (2018) 89–159.

[6] OSQAR collaboration, *New exclusion limits on scalar and pseudoscalar axionlike particles from light shining through a wall*, *Phys. Rev. D* **92** (2015) 092002 [1506.08082].

[7] *Proceedings, 11th Patras Workshop on Axions, WIMPs and WISPs (Axion-WIMP 2015)*, DESY-PROC, (Hamburg), pp. 1–251, 11th Patras Workshop on Axions, WIMPs and WISPs, Zaragoza (Spain), 22 Jun 2015 - 26 Jun 2015, Verlag Deutsches Elektronen-Synchrotron, Jun, 2015, DOI.

[8] M.D. Ortiz *et al.*, *Design of the ALPS II optical system*, *Phys. Dark Univ.* **35** (2022) 100968 [2009.14294].

[9] A. Hallal, G. Messineo, M.D. Ortiz, J. Gleason, H. Hollis, D. Tanner *et al.*, *The heterodyne sensing system for the ALPS II search for sub-ev weakly interacting particles*, *Physics of the Dark Universe* **35** (2022) 100914.

[10] R. Shah, K.-S. Isleif, F. Januschek, A. Lindner and M. Schott, *TES detector for ALPS II*, *Proceedings of The European Physical Society Conference on High Energy Physics — PoS(EPS-HEP2021)* (2022) .

[11] K.-S. Isleif, *The Any Light Particle Search experiment at DESY*, 2202.07306.

[12] K. Irwin and G. Hilton, *Transition-edge sensors*, in *Cryogenic Particle Detection*, (Berlin, Heidelberg), pp. 63–150, Springer Berlin Heidelberg (2005), DOI.

[13] R. Shah, K.-S. Isleif, F. Januschek, A. Lindner and M. Schott, *Characterising a Single-Photon Detector for ALPS II*, *Journal of Low Temperature Physics* **209** (2022) 355.

[14] J.A. Rubiera Gimeno, K.-S. Isleif, F. Januschek, A. Lindner, M. Meyer, G. Othman *et al.*, *The TES detector of the ALPS II experiment*, *Nuclear Instruments and Methods in Physics Research Section A: Accelerators, Spectrometers, Detectors and Associated Equipment* **1046** (2023) 167588.

[15] M. Meyer, K. Isleif, F. Januschek, A. Lindner, G. Othman, J.A. Rubiera Gimeno *et al.*, *A first application of machine and deep learning for background rejection in the ALPS II TES detector*, *Annalen der Physik* 2200545.

[16] A. Lita, A. Miller and S. Nam, *Energy collection efficiency of tungsten transition-edge sensors in the near-infrared*, *Journal of Low Temperature Physics* **151** (2008) 125.

[17] A. Lita, A. Miller and S. Nam, *Counting near-infrared single-photons with 95% efficiency*, *Optics express* **16** (2008) 3032.

[18] M. Schmidt, M. Helversen, M. López, F. Gericke, E. Schlottmann, T. Heindel *et al.*, *Photon-number-resolving transition-edge sensors for the metrology of quantum light sources*, *Journal of Low Temperature Physics* **193** (2018) .

[19] M. López, R. Ebling, H. Hofer, B. Rodiek and S. Kück, *Single-photon avalanche detector calibration at PTB*, in *2018 Conference on Precision Electromagnetic Measurements (CPEM 2018)*, pp. 1–2, 2018, DOI.

[20] C. Schwemmbauer, Y. Hochberg, K.-S. Isleif, F. Januschek, B.V. Lehmann, A. Lindner *et al.*, *Direct dark matter searches using ALPS II's TES detection system*, *Proceedings of The European Physical Society Conference on High Energy Physics — PoS(EPS-HEP2023)* (submitted to journal) .